TORSIONAL PERFORMANCE OF WIND TURBINE BLADES – PART II: NUMERICAL VALIDATION

Kim Branner*, Peter Berring*, Christian Berggreen and Henrik W. Knudsen****
***Wind Energy Department, Risø National Laboratory, Technical University of Denmark**
****Department of Mechanical Engineering, Technical University of Denmark**

Keywords: *Wind turbine blade, bending, torsion, finite element analysis*

Abstract

The present work investigates how well different finite element modeling techniques can predict bending and torsion behavior of a wind turbine blade. Two shell models are investigated. One model has element offsets and the other has the elements at the mid-thickness surfaces of the model. The last two models investigated use a combination of shell and solid elements.

The results from the numerical investigations are compared with measurements from testing of a section of a full-scale wind turbine blade. It is found that only the combined shell/solid models give reliable results in torsion. Both the combined shell/solid models and the shell model with element offsets are found to give reliable bending results. For the combined shell/solid models, convergence tests show that it is necessary to have 3 solid elements through the thickness of the sandwich cores and the adhesive bonds.

1 Introduction

Modern wind turbine blades are constructed using a combination of different materials. Typically glass fiber reinforced plastic is used for most of the structure, with most of the fibers in the longitudinal direction to limit tip deflections. Carbon fibers are used increasingly for very large blades to increase the stiffness of the blade further.

As wind turbines increase in size the torsional eigenfrequency becomes lower and the torsional mode may couple with some of the lower bending modes. This can lead to catastrophic collapse due to flutter instability. For larger wind turbines it therefore becomes gradually more important to be able to make reliable prediction of the torsional behavior of the blade and to calculate any structural couplings that may exist, such as the bend-twist coupling.

Earlier work has shown limited correlation between the torsional response obtained by numerical structural models and measurements. In [1] the response of a beam and a shell finite element (FE) model was compared. In general, the comparison of the torsional response of the two models showed poor correlation, both regarding the torsional eigenfrequency and eigenmode, and regarding the torsional contents of the flapwise and edgewise bending modes. In [2] the response of the numerical models from [1] was compared with a number of measured modal modes and also here the correlation related to torsional responses was limited including the 1st torsional mode and especially for the higher modes. In predicting torsional behavior, pitfalls associated with the use of offset nodes for layered shell elements in FE analysis was reported in [3].

The work in this paper deals with FE modeling techniques to overcome these uncertainties in determining reliable torsional responses. The numerical results are compared with results from the experimental investigation of a full-scale wind turbine blade section, to be found in PART I of this paper [4].

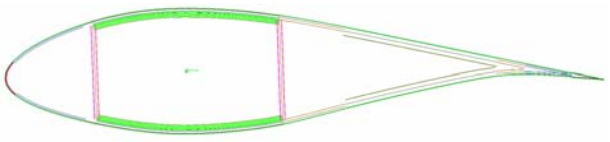

Fig. 1. Outer surface FE-model with material offset

2 Numerical Models

Four finite element models were created and analyzed during this work.

1. Outer surface shell model – using shell element offset.

2. Mid-thickness shell model.
3. Combined shell/solid model.
4. Modified shell/solid model with extra UD-layers.

All models are created using MSC.Patran as pre- and post processor. MSC.Nastran is used as the solver and all analyses are linear with respect to both material and geometry. The small displacements analyzed are found to cause negligible non-linearities.

2.1 Outer Surface Shell Model

The outer surface model of the blade section is a shell model based on the outer surface, meaning that the shell elements are located on the physical outer surface of the aerodynamic shell. The material is then offset in order to locate it at the correct physical position, see Fig. 1. This type of model is typically used for practical design of wind turbine blades today.

2.2 Mid-thickness Shell Model

The mid-thickness model is also created from the geometry of the aerodynamic shell. However, here the shell elements are located at the mid-plane for the different parts of the cross section. The different material thicknesses in the cross section imply that the FE shell will not have a continuous surface like the outer surface model. The discontinuous surfaces are connected by rigid (fixed) elements. These rigid elements are capable of transferring all displacements and rotations from one node to another without deforming.

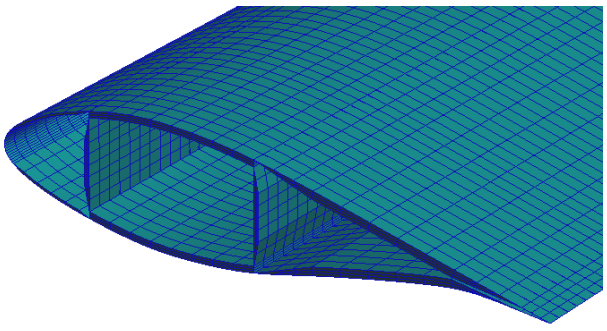

Fig. 2. Meshed part of shell/solid FE-model

2.3 Combined Shell/Solid Model

The combined shell/solid model is constructed based on the following surfaces representing the blade section:

- Outer aerodynamic surface (outer sandwich skins).
- Inner sandwich skins in the leading and trailing part of the blade.
- Leading and trailing edge.
- Web sandwich skins.
- Spar caps.

After creating the surfaces, the solids are then created from two opposing surfaces. The solids represent the following:

- Sandwich core in the leading and trailing part of the blade.
- Sandwich core in the webs.
- Adhesive bonds between the aerodynamic shell and the spar.

Layered shell elements are then used to represent the composite laminates on both sides of the solids.

2.3.1 Mesh

The surfaces are meshed with 8-noded shell elements (Quad8) and the solids are meshed with 20-noded solid elements (Hex20). See meshed model in Fig. 2.

A Quad4/Hex8 configuration reduces the number of degrees of freedom (DOF), but this configuration was not used because of the limited aspect ratios and possible problems with shear locking.

It is usually recommended that the aspects ratio is below 2 when working with Quad4/Hex8 elements. However, this is not practical when meshing the leading edge. The leading edge requires a very fine mesh in the transverse direction because of the high curvature. If the leading edge is meshed with Quad4 elements, then the element size must also be very fine in the longitudinal direction to keep the aspects ratio below 2. This increases the number of nodes and therefore also increases the solving time.

The maximum aspect ratio for Quad8/Hex20 elements is usually 10-12 which means that the leading edge can be meshed with longer elements and thereby reduces the number of nodes in the longitudinal blade direction.

The necessary mesh density for the blade section is determined from a flapwise-, edgewise- and torsional convergence test by examining the cross sectional displacements and rotations. In general, a relative coarse meshed FE-model can give

accurate global displacement results, but a much finer mesh is required for analyzing stresses and strains in the structure.

The shell/solid FE-model consists of a mesh with 74 elements circumferentially, 175 elements longitudinally and the convergence tests show that it is necessary to have 3 solid elements through the thickness of the sandwich cores and the adhesive bonds. The model has approximately 600.000 degrees of freedom.

2.3.2 Loads and Boundary Conditions

It is generally difficult to develop a good numerical model of the real boundaries experienced by the blade section in the experiments. Instead of trying to model the real experimental boundary conditions an alternative approach is applied.

The FE models are fixed at the second support clamp and loaded at the load clamp approximately 6m from the fixed end, see Fig. 3. For both the numerical and the experimental results, the cross sectional displacements and rotations are determined at each half meter using least squares algorithms. See a more comprehensive description in [4].

The results are compared from 0.5m to 5.5m from the fixed end. This is done by subtracting the measured/predicted deflections and rotations for the first cross section from all the other cross sections. The first section can then be considered as fully fixed and clamped for both the experiments and the FE-model predictions. The longitudinal coordinate (z) is in the following set to zero at this first section.

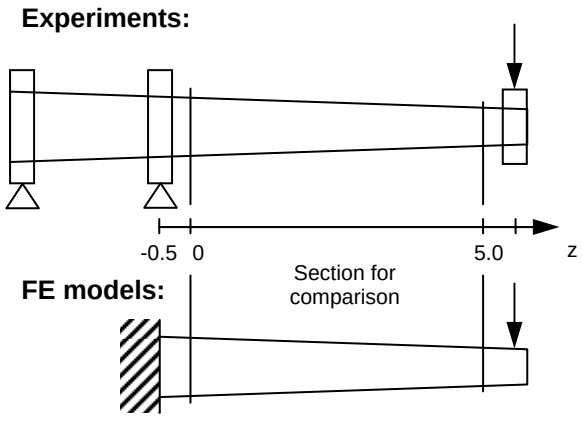

Fig. 3. Boundary conditions and loading of FE models compared with experimental setup.

2.3.3 Lay-up

The FE-model is “laminated” with the MSC.Patran module, Laminate Modeler. In Laminate Modeler the lay-up is entered with data for each ply in the same stacking sequence as it would be placed in the blade production.

The initial application point, fiber orientation and extent of each ply are specified, and Laminate Modeler determines the fiber orientations over the full extent of the ply. When all plies are modeled and stacked into a laminate, Laminate Modeler determines the equivalent properties of the lay-up for each shell element.

2.3.4 Adhesive Bond Modification

The spar caps are modeled with mid-thickness shell elements. The correct location of these shell elements is critical in order to have an accurate model. The shell elements in the spar caps are connected to the aerodynamic shell by adhesive bonds.

Because of the considerable thickness of the spar caps, it is therefore necessary to model the adhesive bond between spar cap and aerodynamic shell about three times thicker than the real bonds, in order to have the correct location of the shell elements.

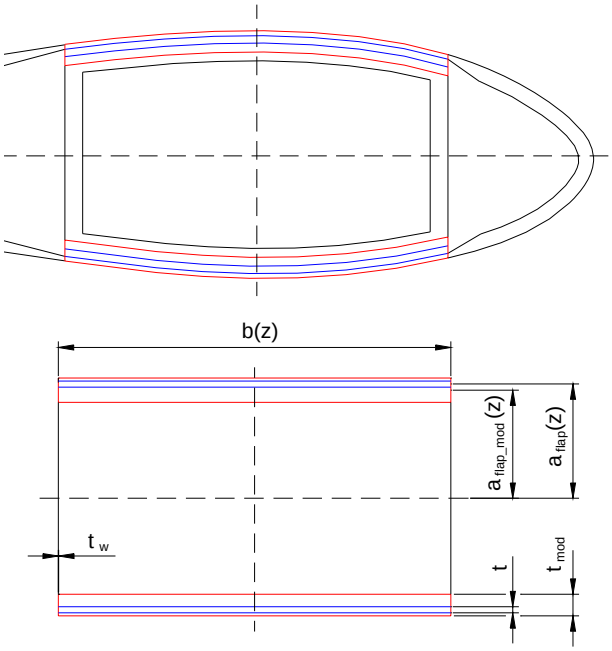

Fig. 4. The blue lines show the real bond and the red shows the modified bond that is used in the shell/solid FE-model. Below, simplified adhesive bond used for calculating the modified E- and G-modulus that are used in the FE-model

A modification of the adhesive properties is therefore needed, in order to have the modeled thick adhesive bond behave in the same way as the real thinner bond. The used modification is based on the

bending and torsional stiffness of the adhesive bond itself.

Since the adhesive bond has a significant influence on the section stiffness, then a set of modified E- and G-moduli were determined. The new moduli together with the modeled bond should give the same sectional stiffness as for the original blade as shown in Eq. 1.

$$E_{flap\_\mathrm{mod}}(z) = \frac{E_{flap} I_{flap}(z)}{I_{flap\_\mathrm{mod}}(z)}$$

$$E_{edge\_\mathrm{mod}}(z) = \frac{E_{edge} I_{edge}(z)}{I_{edge\_\mathrm{mod}}(z)} \qquad (1)$$

$$G_{\mathrm{mod}}(z) = \frac{GJ(z)}{J_{\mathrm{mod}}(z)}$$

It is important to know the location and orientation of the principal axes in order to determine the area moment of inertia (I) for the adhesive bonds. In this case, it is assumed that the elastic center is placed in the center of the spar and it is assumed that the flapwise principal axis is perpendicular to the shear webs, see Fig. 4.

Both the original and the modified adhesive bonds have the same width ($b(z)$) and the same curvature around the z-axis. This mean that the distances $a_{flap}(z)$ and $a_{flap\_\mathrm{mod}}(z)$ are the same and a simplified rectangular shape can therefore be used for calculating the moment of inertia.

By analyzing the adhesive bond as a rectangular tube, the moments of inertia and the cross sectional torsion factor can be determined as shown in Eq. 2 and Eq. 3 respectively.

$$I_{flap} = 2\left(\frac{1}{12} b(z) t^3 + b(z) t a_{flap}(z)^2\right)$$

$$I_{edge} = 2\left(\frac{1}{12} b(z)^3 t + b(z) t a_{edge}(z)^2\right) \qquad (2)$$

$$I_{flap\_\mathrm{mod}} = 2\left(\frac{1}{12} b(z) t_{\mathrm{mod}}{}^3 + b(z) t_{\mathrm{mod}} a_{flap\_\mathrm{mod}}(z)^2\right)$$

$$I_{edge\_\mathrm{mod}} = 2\left(\frac{1}{12} b(z)^3 t_{\mathrm{mod}} + b(z) t_{\mathrm{mod}} a_{edge\_\mathrm{mod}}(z)^2\right)$$

$$J(z) = \frac{2t\, t_w b(z)^2 h(z)^2}{b(z) t_w + h_0(z) t_{\mathrm{mod}}}$$

$$J_{\mathrm{mod}}(z) = \frac{2 t_{\mathrm{mod}} t_w b(z)^2 h_{\mathrm{mod}}(z)^2}{b(z) t_w + h_1(z) t_{\mathrm{mod}}} \qquad (3)$$

with

$$h(z) = 2a_{flap}(z)$$

$$h_{\mathrm{mod}}(z) = 2a_{flap\_\mathrm{mod}}(z)$$

The expression for the torsional factor J/J_{mod} is taken from [5].

As mentioned earlier, the adhesive bond is analyzed as a rectangular tube with the flange thicknesses t/t_{mod} and the web thickness t_w. It is necessary to define a web thickness and in this case, it is set to 10^{-8} m. If a web thickness is not defined then the expression will be zero, but by setting the web thickness to a small value then this dependence is eliminated and the webs will not contribute to the overall torsional factor.

2.4 FE-modeling of the Extra UD-layers

The original blade section is modified and four layers of UD1200 are laminated on the pressure and suction side in order to create a more measurable flapwise bend-twist coupling.

The extra UD layers are modeled with solid elements on top of the existing outer surface shell elements. The extra UD layers are meshed with 20-noded solid elements (Hex20) and 1 solid element is used through the thickness. The total number of DOF's for the FE-model increase from 600.000 to 700.000 with the additional solid elements.

3 Numerical Validations

Results from three load cases (flapwise bending, edgewise bending and torsion) using the three FE models are compared with experimental results for the original blade section. Extra UD layers are then added to the blade to introduce a higher bend-twist coupling. Results from two load cases (flapwise bending with and without torsion) are then compared with experimental results using a combined shell/solid FE model. See a thorough description of the experiments in [4].

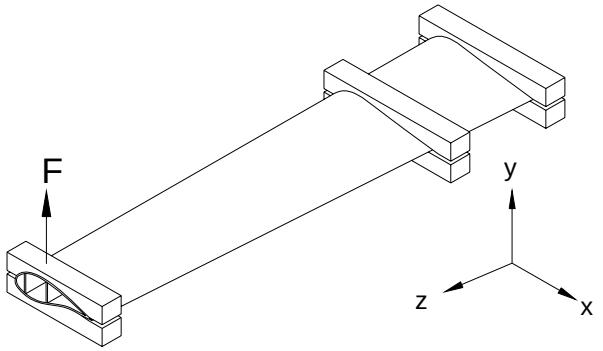

Fig. 5. Flapwise bending of blade section.

3.1 Flapwise Bending

The flapwise bending test is performed by applying a point load of 3923N in the y-direction at the end. See load condition in Fig. 5 and comparison between numerical and experimental results in Fig. 6.

3.1.1 Experiment vs. Outer Surface Shell Model

The numerical predicted flapwise displacement (disp. y-direction) is in excellent agreement with the experimental results; the deviation is only about 1.5%. The rotation about the x-axis is also in excellent agreement with the experimental results; the deviation is only about 1.6%.

For the rotation about the z-axis the agreement is relatively good. If it is assumed that the shear center is located at the center of the spar, then it can be concluded that both the numerical and experimental bend-twist coupling (flapwise) are of very limited size. The deviation in the rotation about the z-axis may be due to uncertainties regarding the hydraulic press, experimental measuring accuracy and experimental setup.

3.1.2 Experiment vs. Mid-thickness Shell Model

In general, the numerical results are in good agreement with the experimental results for the inner 3m of the blade section, but further out the numerical results starts to deviate.

This is the case for all the displacements and rotations which indicates that there is a general problem with the numerical model. The rotation about the x-axis drops when going from 3 – 3.5m and again when going from 4 – 4.5m.

The blade section has ply drops in the spar caps at these two locations and this is modeled in the mid-thickness FE-model by dividing the spar cap into three areas with different laminate properties. The three spar cap areas represent three different mid-thicknesses which are connected by rigid elements across the cap (see Fig. 7).

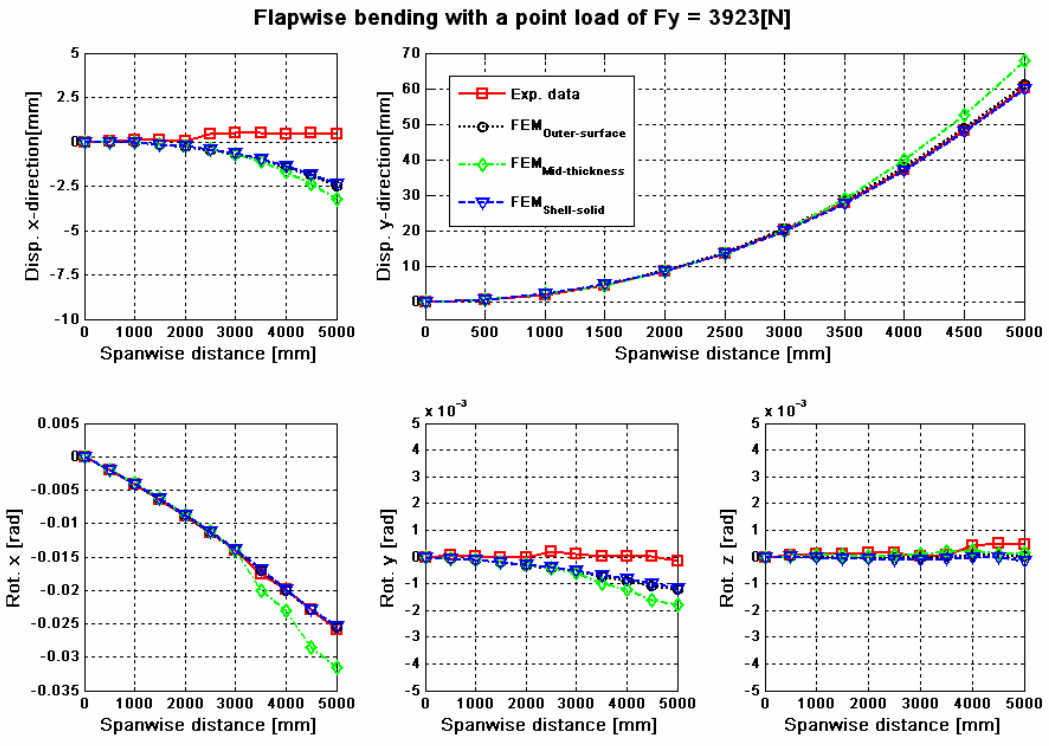

Fig. 6. Flapwise bending: Comparison of numerical and experimental results.

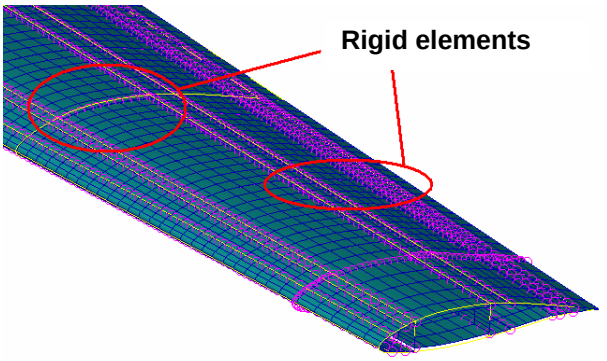

Fig. 7. Rigid elements (violet) in the mid-thickness FE-model.

The FE-model was also modified by deleting the rigid elements and then connecting the adjacent shell elements at the mid-point of the deleted rigid elements. This approach is questionable, but was chosen in order to investigate if the problem could be isolated to be due to the rigid elements in the spar caps. This modified mid-thickness model was in relative good agreement with the experimental results over the whole length, and it is therefore indicated that using rigid elements over ply drops is not a good practice.

3.1.3 Experiment vs. Combined Model

The flapwise bending behavior of the combined shell/solid FE-model is almost identical to the flapwise bending behavior of the outer surface FE-model. The numerical prediction is in excellent agreement with the experimental results. The deviation between the numerical and experimental results for the displacement in the y-direction is about 1% and about 2% for the rotation about the x-axis.

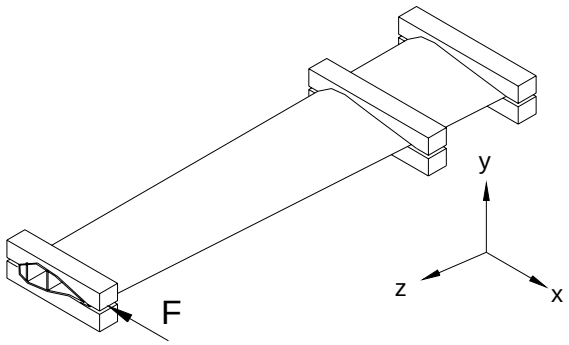

Fig. 8. Edgewise bending of blade section.

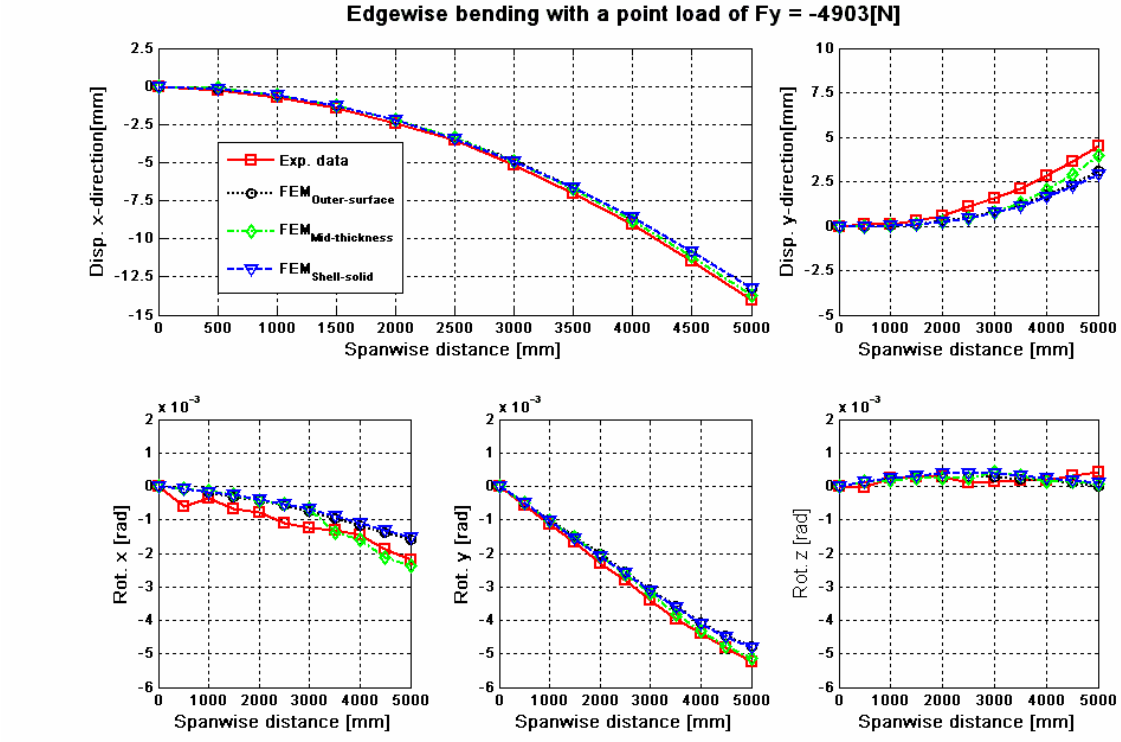

Fig. 9. Edgewise bending: Comparison of numerical and experimental results.

3.2 Edgewise Bending

The edgewise bending test was performed by applying a point load of 4903N in the negative x-direction at the end. See load condition in Fig. 8 and comparison between numerical and experimental results in Fig. 9.

3.2.1 Experiment vs. Outer Surface Shell Model

The numerical predicted edgewise displacement (disp. x-direction) is in relative good agreement with the experimental results; the deviation is about 6%. Also the rotation about the y-axis is in relative good agreement with the experimental results; the deviation is about 8%.

For the displacement in the y-direction and the rotation about the x-axis the deviation is about 30 - 40%. The agreement between the numerical and experimental results for the rotation about the z-axis is relative good for the inner 2m, but for the outer 3m some deviation is traceable. The experimental results are very small and not well defined so the rotation about the z-axis is somewhat unstable along the blade. The deviation between numerical and experimental results could therefore be due to uncertainties regarding the measuring accuracy.

3.2.2 Experiment vs. Mid-thickness Shell Model

The edgewise bending behavior (x- and y-disp. and x-, y- and z-rot.) of the mid-thickness FE-model is almost identical to that of the outer surface and shell/solid FE-models for the inner 3m.

But again, the mid-thickness FE-model starts to deviate at 3m span which especially can be seen on the plots of the y-displacement and the x-axis rotation (flapwise). This behavior is due to the problems with the rigid elements as described earlier. The same behavior can also be seen in the plots of the displacement in the x-direction and the rotation about the y-axis.

3.2.3 Experiment vs. Combined Model

Again, the edgewise bending behavior of the shell/solid FE-model is almost identical to that of the outer surface FE-model. The conclusions for the comparison of the shell/solid model with the experimental results are therefore the same as for the outer surface model. The shells were not created with shell element offsets, so the problem with poor bending results when the radius/thickness ratio is low was eliminated with this FE-model.

The deviation between the numerical and experimental results for the displacement in the x-direction is about 6% and about 8% for the rotation about the y-axis. The deviation between the numerical and experimental results for the displacement in the y-direction is about 40 - 50% and about 45% for the rotation about the x-axis.

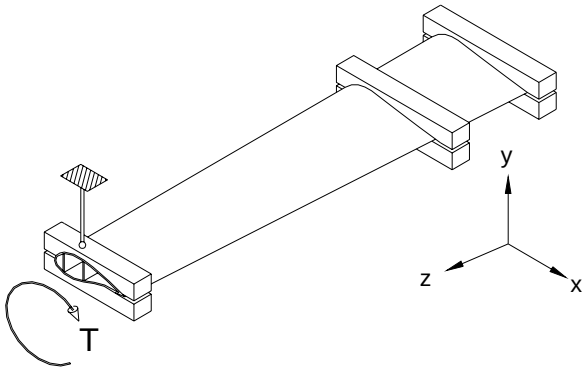

Fig. 10. Locked torsion of blade section.

3.3 Locked Torsion

The numerical locked torsion test is performed by locking the tip cross section in a point directly over the center of the spar. This point cannot move in the vertical plane, but is able to move in the horizontal plane in a circular arc movement and is also able to rotate about this point. A torsional moment of 3408Nm was applied at the end. See load condition in Fig. 10 and comparison between numerical and experimental results in Fig. 11.

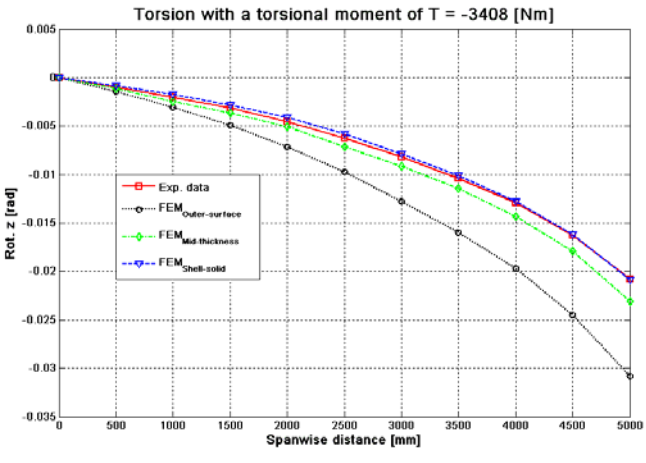

Fig. 11. Comparison between numerical and experimental results for the twist angle

3.3.1 Experiment vs. Outer Surface Shell Model

The agreement between the numerical and experimental results is very poor and the deviation is about 32%. The major part of this disagreement is found to be due to the offset configuration of shell

elements. This configuration has serious problems with modeling correct torsional behavior as can be seen in Fig. 11.

3.3.2 Experiment vs. Mid-thickness Shell Model

The agreement between the numerical and experimental results for the rotation about the z-axis is better than for the outer surface shell model but still the deviation is about 10 - 12%. The major reason for this disagreement is probably due to the rigid elements that connect the shell elements in the areas with different material thicknesses.

3.3.3 Experiment vs. Combined Model

The agreement between the numerical and experimental results for the rotation about the z-axis (twist) is generally very good. The deviation is only about 1 – 4% on the outer 3.5m of the blade section.

The FE-model is not twisting as much as the real blade in the experiment and the deviation for the inner 1.5m is about 5 – 9%. This deviation could be due to:

- Effects from the boundary conditions in the FE-model. The fixed end of the blade section cannot warp when the blade is subjected to torsion and the torsional stiffness could therefore increase considerably when this out-of-plane distortion is restrained.
- The experimental measuring accuracy.
- The hydraulic press was not perfectly aligned with the vertical plane.

3.4 Flapwise Bending of Modified Blade

This load condition is similar to that of the original blade reported in Section 3.1. A point load of 9808N in the y-direction was applied at the end. See load condition in Fig. 5 and comparison between numerical and experimental results in Fig. 12.

The numerical predicted flapwise displacement (disp. y-direction) is in good agreement with the experimental results; the maximum deviation is about 3.5%. The rotation about the x-axis is also in good agreement with the experimental results; the maximum deviation is about 5%.

The agreement between the numerical and experimental results for the rotation about the z-axis is very good for the inner 2.5m, but the FE-model deviates more from the experimental results for the outer 2.5m – the maximum deviation is about 9% at the tip.

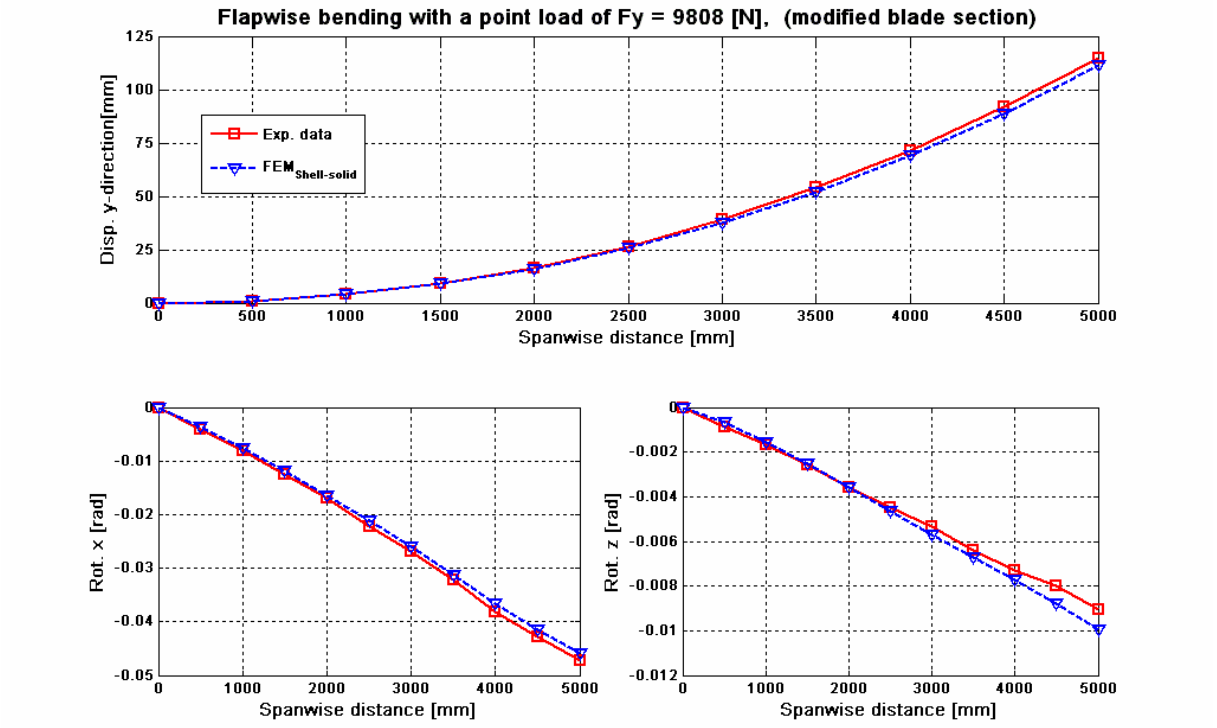

Fig. 12. Flapwise bending of modified blade: Comparison of numerical and experimental results.

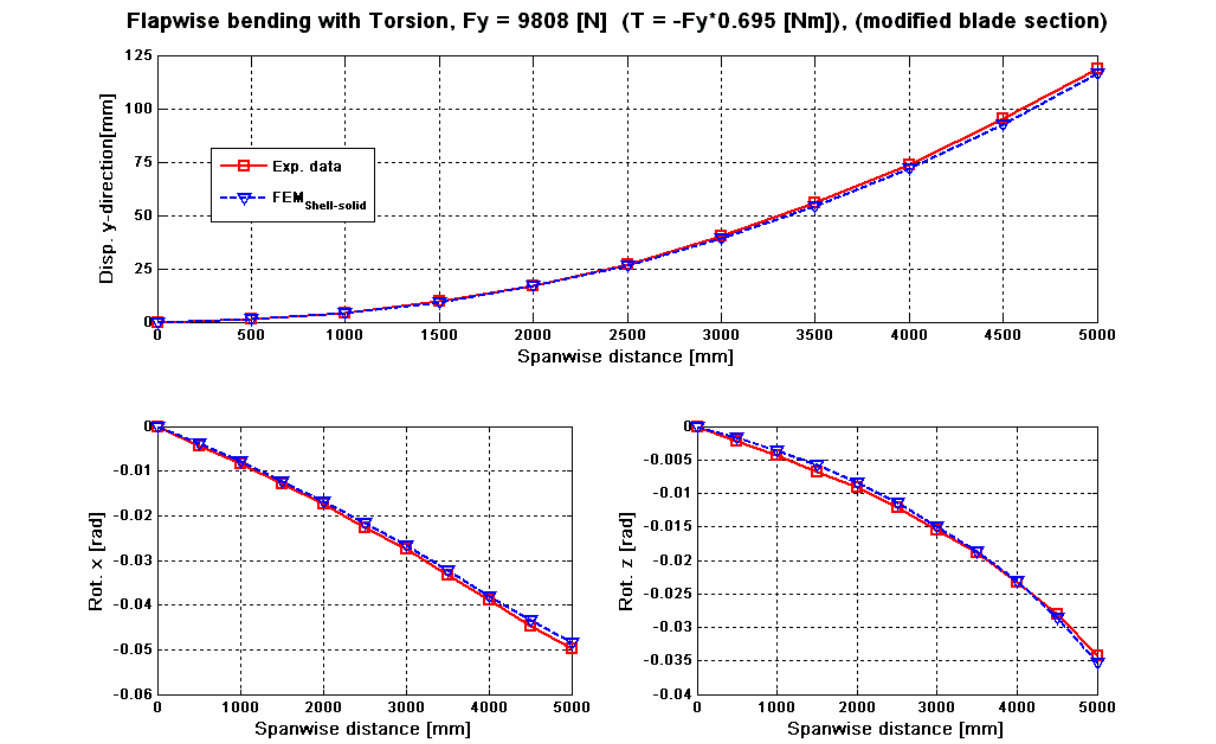

Fig. 13. Combined flapwise bending and torsion for modified blade: Comparison of numerical and experimental results.

The FE-model is generally twisting more than found in the experiment, which could be due to boundary conditions not included in the model. The flapwise tip load is applied by a hydraulic press and the contact from the press could restrain the free tip twist of blade section during the experiment. The FE-model is not twisting as much as seen in the experiment for the inner 1.5m and this could be due to effects from the boundary conditions. Again, torsion related warping is restrained in the numerical model in the fixed end which is not the case during the experiment.

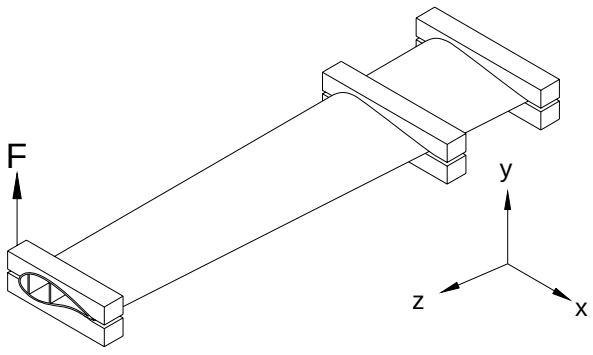

Fig. 14. Flapwise bending and torsion of blade section.

3.5 Flapwise Bending and Torsion of Modified Blade

The flapwise bending and torsion test is performed by applying a point load of 9808N in the y-direction with an offset of 0.7m at the end. The load condition is shown in Fig. 14 and the comparison between numerical and experimental results in shown in Fig. 13.

The numerical predicted flapwise displacement (disp. y-direction) is in good agreement with the experimental results; the maximum deviation is about 2%. Also the rotation about the x-axis is in good agreement with the numerical results; the maximum deviation is about 3.4%. For the rotation about the z-axis the experimental twisting is somewhat larger than the numerical twisting for the inner 3m, but the global twist is in good agreement; the deviation is about 3%.

The deviation for the inner 3m is probably again due to the restraint torsional warping, which increases the torsional stiffness of the FE-model. Overall, it can be concluded that there is a very good agreement between the numerical and experimental

results for the flapwise bending and torsion load case.

4 Conclusions

It is found that accurate flapwise bending results and relatively accurate edgewise bending results can be obtained with the outer-surface FE-model. However, care should be taken with using shell element offset, if the radius/thickness ratio is low. It is also found that the outer surface FE-model is not capable of modeling accurate torsional behavior and bend-twist couplings. The deviation between the numerical and experimental results for the twist angle is as high as 32%.

It is found that the mid-thickness FE-model is incapable of modeling accurate flapwise and edgewise bending, when the model has details like ply-drops in the spar cap. Using rigid elements to connect regions with different material thickness cannot in general be recommended.

Finally, by comparing results from the experiments with the global displacements and rotations for the combined shell/solid FE-models, it can be concluded that the shell/solid model is reliable in modeling accurate flapwise, edgewise and torsional behavior. For this shell/solid model, convergence tests show that it is necessary to have 3 solid elements through the thickness of the sandwich cores and the adhesive bonds. Also, by comparing results from the shell/solid model of the modified blade section with the experiments, it can be concluded that this FE-model type can establish a reliable prediction of the bend-twist coupling.

The shell/solid model is more detailed and accurate than the two shell models. The size of the shell/solid model is also considerable larger and therefore more time consuming to analyze.

References

[1] Madsen H.A. (editor) “Research in aeroelasticity – EFP-98” (in Danish). Risø-R-1129(DA), Risø National Laboratory, Roskilde, Denmark, 1999.

[2] Larsen G.C. “Modal analysis of wind turbine blades”. Risø-R-1181(EN), Risø National Laboratory, Roskilde, Denmark, 2002.

[3] Laird D.L., Montoya F.C. and Malcolm D.J. “Finite element modeling of wind turbine blades”. *Proceedings of AIAA/ASME Wind Energy Symposium*, Reno, Nevada, USA, AIAA-2005-0195, pp 9-17, 2005.

[4] Berring P., Branner K., Berggreen C. and Knudsen H.W., “Torsional performance of wind turbine blades – part I: Experimental investigation”. *16th International Conference of Composite Materials*, Kyoto, Japan, July 2007.

[5] Seaburg, P.A. and Carter C.J. “Torsional Analysis of Structural Steel Members”, Steel Design Guide Series 9, AISC, Chicago, IL, USA, 1997.